ISBN: 978-3-95450-247-9 ISSN: 2673-5490 doi: 10.18429/JACoW-IPAC2024-TUPS87

TIME-RESOLVED EVALUATION OF THE TRANSIENT RESPONSES OF CRYSTAL OPTICS TO INSTANTANEOUS HEAT DEPOSITION FOR WAVEFRONT INTEGRITY*

Y. Hong†, B. Yang, and J. Wu SLAC National Accelerator Laboratory, Menlo Park, CA, USA

Abstract

Our focus centres on numerical investigation into the transient response of optics when subjected to instantaneous heat deposition. The heat load deposited onto crystal optics, coupled with the emission of strain waves, has the potential to induce crystal deformation and vibrations. These phenomena carry detrimental consequences for optic performance, particularly in terms of wavefront preservation—an essential criterion for coherent XFEL beams. Our research involves an evaluation of optical performance in terms of the Strehl ratio at delay time. Ultimately, we aim to provide recommendations for establishing upper bounds on pulse energy and repetition rates during XFEL operation. These guidelines will play a pivotal role in optimizing XFEL performance while safeguarding wavefront integrity, thus advancing the capabilities of coherent X-ray beams in scientific and technological applications.

INTRODUCTION

X-ray free-electron lasers (XFELs) have revolutionized various scientific fields by providing ultra-bright and coherent X-ray pulses. However, one of the significant challenges in utilizing XFELs is maintaining the wavefront integrity of the X-ray beams. Thin diamond crystal optics are employed in XFELs due to their excellent thermal, mechanical, and optical properties. However, these optics are susceptible to thermal mechanical response in short time scale, leading to deformation and vibration [1,2]. To determine the effect of the heat load induced deformation, we numerically examine the deformation at delay time at different pulse energy and temperature setting.

METHODS

We consider Gaussian distributed short x-ray pulse impinging the free surface of crystal with pulse energy of E. The gaussian beam size of σ, and the duration of X-ray pulse pass through the crystal ($< ps$) can be considered as instantaneous when compared to the time scale of thermal stress wave propagation. The distribution of pulse energy E can be expressed as (1),

$$\Delta U(x,y,z) = U_0 \exp[-\frac{x^2}{2\sigma_x^2} - \frac{y^2}{2\sigma_y^2} - \frac{z}{Lsin\theta}]$$
$$U_0 = \frac{E(1-C_{tran})}{2\pi\sigma_x\sigma_y Lsin\theta[1-\exp(-z/Lsin\theta)]} \quad (1)$$

, where the L is laser attenuation length at which its intensity is attenuated by a factor of e, $C_{tran}$is transmission, σ_x, σ_y is the transverse beam size, and θ is the incident angle. We define $\sigma_x = \frac{\sigma}{sin\theta}$, and $\sigma_y = \sigma$.

The initial temperature distribution within $T_0(x,y,z)$ from crystal temperature T_c after absorbing ΔU can be calculated (2),

$$\Delta U = \int_{T_c}^{T_0} \rho C_P(T) dT \quad (2)$$

, where ρ is the material density, and $C_P(T)$ is the temperature-dependent specific heat of the crystal, and T_c is the crystal temperature.

The optical performance is evaluated through calculating the Strehl ratio (SR) within the Region of Interests (ROI) at delay time, t. The Strehl ratio is defined as the intensity ratio from an aberrated reflector versus from ideal reflector. The SR can be calculated in terms of the root mean square of phase error Φ induce by the aberrated crystal surface (3) [3].

$$SR = |\exp(i\Phi)|^2 \quad (3)$$

The surface aberration, in this case the height error, Δh induced by the instantaneous heat deposition due to local thermal expansion. The Δh resulted optical path length difference, $L = 2\Delta h \sin\theta$, where θ here is the incident angle. When consider Δh as the stander deviation or RMS value with referencing average heigh within the ROI, the phase error can be written as (4)

$$\Phi = \frac{4\pi\Delta h \sin\theta}{\lambda} \quad (4)$$

When considering Bragg's condition, $\lambda = 2d\sin\theta_B$, where d is interplane distance between reflection plane, $d = \frac{a}{\sqrt{h^2+k^2+l^2}}$, a here is crystal lattice spacing; the $h,\ k,\ l$ and θ_B is the Miller Index and Bragg's angle of the respected reflection plane.

As time evolve, heat dissipate away from hot spot, the Δh decrease over time. The optical performance at time delay can be quantified by substituting the RMS of surface aberration $\Delta h(t)$ at time delay.

$$SR(t) = \exp\left[-\left(\frac{2\pi\Delta h(t)\sqrt{h^2+k^2+l^2}}{a}\right)^2\right] \quad (5)$$

Transient thermal-mechanical analysis to assess the impact of thermal energy release on surface aberration over time.

The thermal contact conductance (TCC) determines the temperature difference between the crystal sample and the mounting, and it can vary significantly depends on the contact condition, intermedia material, and temperature as suggested in [4, 5].

* Work supported by the LCLS Photon R&D funds, SLAC PD funds & U.S. Department of Energy Office of Science grant SLAC FWP 100966.
† hong274@slac.stanford.edu

ISBN: 978-3-95450-247-9 ISSN: 2673-5490 doi: 10.18429/JACoW-IPAC2024-TUPS87

The characteristic time, which can be used to estimate the time for temperature redistribution [6], can be calculated with (6) by using the dimension of the ROI, L, and thermal diffusivity $\alpha(T)$

$$\tau = \frac{L^2}{\alpha(T)} \quad (6)$$

For diamond, the $\alpha(T)$ is significantly higher than silicon across temperature range. For instance, at room temperature, the α_{Si} is ~ 1 cm^2/s [7], while diamond is roughly an order higher α_C is ~ 11 cm^2/s; at cryogenic temperature of 100K, the diffusivity difference between the two materials becomes larger, for silicon ~ 22-28 cm^2/s, while α of diamond can be as high as 700 cm^2/s.

Due to the high diffusivity of diamond at cryogenic temperature, the temperature difference between can be treated as constant when running at fixed repetition rate.

RESULT ANALYSIS

For this work, we adapted a typical sample mounting scheme with cryogenic cooling capability, as shown in Figure 1. The diamond sample is clamped between leaf spring clamper and mounting base. The aft end of the leaf spring clamper is held by 2 M2 machine screws. The material of each part is listed in Table 1

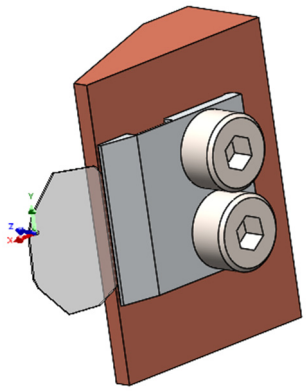

Figure 1: crystal – sample holder assembly.

Table 1: Material List for the Numerical Simulation Model

Items	Material
Mount	OFHC Copper
Clamp	Stainless Steel
M2 screw	Stainless Steel
Sample	Type IIa diamond

The diamond sample used in our simulation is untreated in its raw form, it is roughly 7×7 mm in size octagonal shape, and roughly 100 µm thick. The x-y-z coordinate marks the region of interest (ROI) on the diamond sample, where the z-direction aligned with the thickness of sample, where $z = 0$ is the incident surface. The ROI is chosen to be at a distance from where it's clamped, with the intention of minimizing the effect from clamping strain. The size of the ROI is 3 times of the σ_y. To reduce the model size, the lower end (y - direction, parallel to the x-z plane) of the mounting base is omitted, and a fixed temperature T_M is assigned in place.

For this analysis, we consider 9.831 keV X-ray pulse with pulse energy from 0.1 to 2 mJ and a fixed pulse size of 300 µm FWHM ($\sigma = \frac{D_{FWHM}}{2\sqrt{2ln2}}$). The pulse impinging diamond (400) plane at its Bragg's condition, θ_B ~ 45°, absorption length is ~ 1500 µm and the X-ray transmission is ~ 0.90. We assume the initial temperature of the diamond factored in the temperature off-set due to the TCC. We assumed InGa eutectic is applied between the diamond and the OFHC copper mount, which the thermal contact conductance is 45 W/(cm^2-K) [8].

The initial temperature rise is calculated with method formulated in prior chapter using temperature dependent thermal properties. Then, the initial temperatures were imported into ANSYS (Workbench 2022 R2) transient thermal module and applied as initial condition within the volume of the crystal, such as shown in Figure 2. the calculation carried up to 1 ms. The initial temperature change is summarized in Table 2.

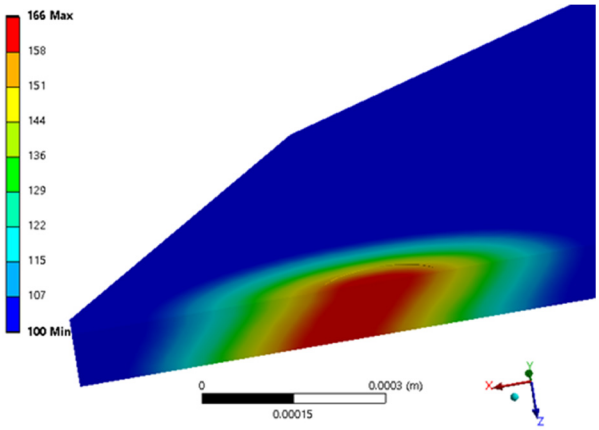

Figure 2: Cut-away view of initial temperature distribution of E = 1mJ D_{FWHM} = 300 µm at 9.831keV of cryogenic temperature case.

Table 2: Maximum Initial Temperature Rise

Pulse energy (µJ)	100	200	500	1000	2000
ΔT_{max} (100K)	15	25	45	66	91
ΔT_{max} (300K)	0.7	1.4	3.5	6.9	14

For comparison, at different initial temperatures, it is obvious that in cryogenic condition, the time scale of recovery from thermal deformation is shorter. And they are in the same range of the characteristics time estimation mentioned in prior section. It is worth noting that in the cryogenic condition cases, the recovery time of high pulse energy is longer than the low energy pulse. This is due to the high energy pulse will generate a higher initial temperature distribution, and the thermal diffusivity is negatively correlated with increase in temperature, the heat effectively

ISBN: 978-3-95450-247-9 ISSN: 2673-5490 doi: 10.18429/JACoW-IPAC2024-TUPS87

'trap' for longer time within the heated region. As for the room temperature cases, although high pulse energy still generates a higher temperature within the distribution than low energy pulse does, the difference in diffusivity is small.

The temperature distribution at time delays were then imported into static structural for deformation (Uz) calculations. The deformation decreases as heat dissipates into the surrounding volume. We calculated RMS (with reference form 0) of the z-component of deformation within the ROI for each time delay Figure 3. The results indicate that the heat load leads to crystal deformations which adversely affect the optic's ability to preserve the wavefront of the coherent XFEL beam.

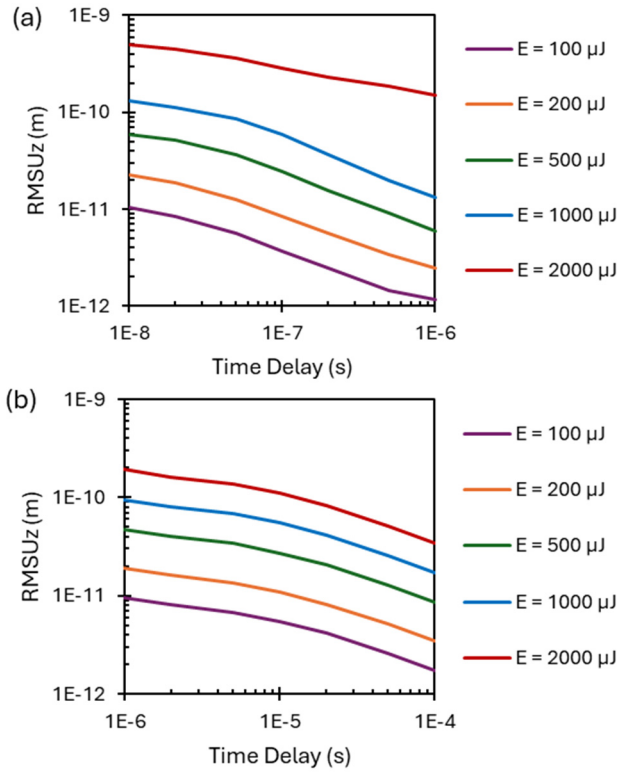

Figure 3: RMS of deformation within ROI at delay time at (a) T_c = 100K and (b) T_c = 300K

The illustrate the consequences of the thermal deformation on the optical performance, we evaluate the Strehl ration with equation (5) by equating Δh to the deformation RMS at time delays. In Figure 4, we mapped the calculated Strehl ratio (color bar) in terms of the pulse energy and repetition rate (invers of delay time). For Strehl ratio at its lower end, for example at SR = 0.1, the focus becomes blurred, the beam intensity at the center of the ROI decreases to 1/10 of the ideal condition.

The result also indicates that by cooling the crystal from room temperature to 100 K, at a fixed pulse energy, purely on the thermal point of view, the 'allowable' repetitions rate can be nearly two orders higher than room temperature.

The Strehl ratio calculation considered the deformation in the form heigh error within the ROI. However, the local surface slope as well as strain also impacts the in the reflection quality. Strehl ratio greater than 0.8, or the rms deformation heigh error is less than $\lambda/14$, where the aberration can be considered as small enough not to significantly distort the image.

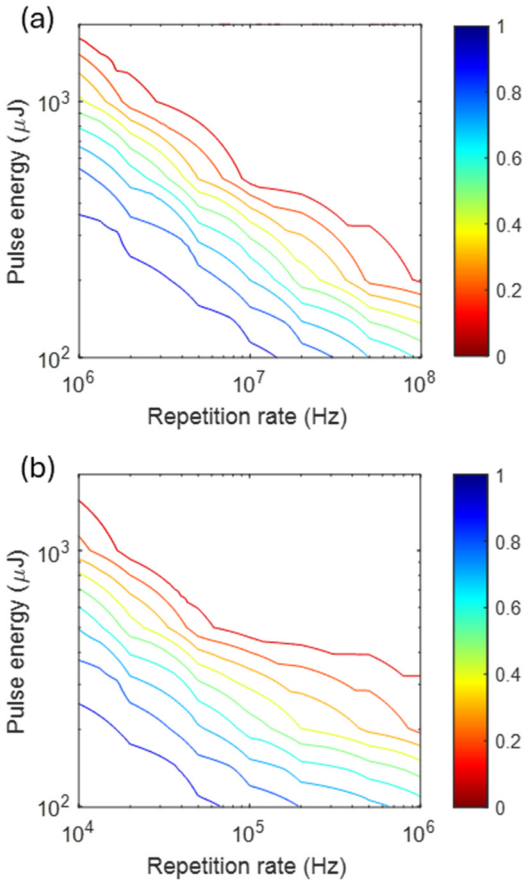

Figure 4: Strehl Ratio within the ROI in terms of repetition rate at (a) T_c = 100K and (b) T_c = 300K

CONCLUSION

In work, we present a numerical study by evaluating the Strehl ratio at time delay of a single pulse using C (400). The findings underscore the critical importance of temperature control in the performance of diamond crystal X-ray optics. The study also highlights the need for integrated temperature control systems tailored to the specific demands of X-ray optics applications. The finding establishes an upper limit on pulse energy and repetition rates to mitigate adverse effects on crystal optics.

REFERENCES

[1] B. Yang, S. Wang, and J. Wu, "Transient thermal stress wave and vibrational analyses of a thin diamond crystal for X-ray free-electron lasers under high-repetition-rate operation," *J. Synchrotron Radiat.*, vol. 25, no. 1, pp. 166–176, Jan. 2018. doi:10.1107/s1600577517015466

[2] I. Bahns, P. Rauer, J. Rossbach, and H. Sinn, "Stability of Bragg reflectors under megahertz heat load at XFELs," *J. Synchrotron Radiat.*, vol. 30, no. 1, pp. 1–10, Jan. 2023. doi:10.1107/s1600577522009778

ISBN: 978-3-95450-247-9 ISSN: 2673-5490 doi: 10.18429/JACoW-IPAC2024-TUPS87

[3] L. Zhang, M. Seaberg, and H. Yavaş, "Towards a wavefront-preservation X-ray crystal monochromator for high-repetition-rate FELs," *J. Synchrotron Radiat*., vol. 30, no. 4, pp. 686–694, Jun. 2023. doi:10.1107/s1600577523004216

[4] Z. Qu, Y. Ma, and J. Wu, "Exploring mounting solutions for cryogenically cooled thin crystal optics in high power density x-ray free electron lasers," *Rev. Sci. Instrum*., vol. 95, no. 5, May 2024. doi:10.1063/5.0191095

[5] M. M. Yovanovich, "Four decades of research on thermal contact, gap, and joint resistance in microelectronics," *IEEE Transactions on Components and Packaging Technologies,* vol. 28, no. 2, pp. 182–206, Jun. 2005. doi:10.1109/tcapt.2005.848483

[6] I. Petrov *et al*., "Performance of a cryo-cooled crystal monochromator illuminated by hard X-rays with MHz repetition rate at the European X-ray Free-Electron Laser," Optics Express, vol. 30, no. 4, p. 4978, Feb. 2022. doi:10.1364/oe.451110

[7] H. R. Shanks, P. D. Maycock, P. H. Sidles, and G. C. Danielson, "Thermal Conductivity of Silicon from 300 to 1400°K," *Physical Review*, vol. 130, no. 5, pp. 1743–1748, Jun. 1963. doi:10.1103/physrev.130.1743

[8] L. Assoufid and A. M. Khounsary, "Contact heat conductance at a diamond-OFHC copper interface with GaIn eutectic as a heat transfer medium," *Rev. Sci. Instrum*., vol. 67, no. 9, pp. 3354–3354, Sep. 1996. doi:10.1063/1.1147400